

# Magnetic resonance peak and nonmagnetic impurities

Y. Sidis<sup>1</sup>, P. Bourges<sup>1</sup>, B. Keimer<sup>2</sup>, L. P. Regnault<sup>3</sup>, J. Bossy<sup>4</sup>, A. Ivanov<sup>5</sup>, B. Hennion<sup>1</sup>, P. Gautier-Picard<sup>1</sup>, G. Collin<sup>1</sup>

<sup>1</sup> *Laboratoire Léon Brillouin, CEA-CNRS, CE-Saclay, 91191 Gif sur Yvette, France.*

<sup>2</sup> *Max-Planck-Institut für Festkörperforschung, 70569 Stuttgart, Germany.*

<sup>3</sup> *CEA Grenoble, Département de Recherche Fondamentale sur la Matière Condensée, 38054 Grenoble cedex 9, France.*

<sup>4</sup> *CNRS-CRTBT, BP 156, 38042 Grenoble cedex 9, France.*

<sup>5</sup> *Institut Laue Langevin, 156X, 38042 Grenoble cedex 9, France.*

Nonmagnetic Zn impurities are known to strongly suppress superconductivity. We review their effects on the spin excitation spectrum in  $\text{YBa}_2\text{Cu}_3\text{O}_7$ , as investigated by inelastic neutron scattering measurements.

## I. INTRODUCTION

In optimally doped  $\text{YBa}_2\text{Cu}_3\text{O}_{6+x}$ , the spin excitation spectrum is dominated by a sharp magnetic excitation at an energy of  $\sim 40$  meV and at the planar antiferromagnetic (AF) wave vector  $(\pi/a, \pi/a)$ , the so-called magnetic resonance peak [1–6]. Its intensity decreases with increasing temperature and vanishes at  $T_c$ , without any significant shift of its characteristic energy  $E_r$ . In the underdoped regime,  $E_r$  monotonically decreases with decreasing hole concentration [7–10], so that  $E_r \simeq 5 k_B T_c$ . Besides, it is possible to vary  $T_c$  without changing the carrier concentration through impurity substitutions of Cu in the  $\text{CuO}_2$  planes. In  $\text{YBa}_2(\text{Cu}_{0.97}\text{Ni}_{0.03})_3\text{O}_7$  ( $T_c=80$  K), the magnetic resonance peak shifts to lower energy with a preserved  $E_r/T_c$  ratio [11].

In optimally doped  $\text{Bi}_2\text{Sr}_2\text{CaCu}_2\text{O}_{8+\delta}$  ( $T_c=91$  K), a similar magnetic resonance peak has been recently observed at 43 meV [12]. Furthermore,  $E_r$  shifts down to 38 meV in the overdoped regime ( $T_c=80$  K) [13], preserving a constant ratio with  $T_c$ :  $E_r \simeq 5.4 k_B T_c$ . Thus, whatever the hole doping, the energy position of the magnetic resonance peak always scales with  $T_c$ .

In underdoped  $\text{YBa}_2\text{Cu}_3\text{O}_{6+x}$  ( $x=0.6, T_c=63$  K,  $E_r=34$  meV), recent INS measurements provide evidence for incommensurate-like spin fluctuations at 24 meV and low temperature (seemingly similar to those observed  $\text{La}_{2-x}\text{Sr}_x\text{CuO}_4$ ) [14,15]. These incommensurate-like spin fluctuations are also observed at higher oxygen concentrations:  $x=0.7$  [16,17],  $x=0.85$  [18]. As a function of temperature [16,18] and energy [18], the incommensurability increases below  $T_c$  with decreasing temperature and decreases upon approaching  $E_r$  in the superconducting state. The results point towards an unified description of both incommensurate spin excitations and magnetic resonance peak in terms of an unique (dispersive) collective spin excitation mode, as predicted in Ref. [19].

In this paper, we review effects of nonmagnetic Zn impurities on the magnetic resonance peak in  $\text{YBa}_2\text{Cu}_3\text{O}_7$ . Among all candidates for substitution to Cu in the  $\text{CuO}_2$  planes of  $\text{YBa}_2\text{Cu}_3\text{O}_7$ , nonmagnetic  $\text{Zn}^{2+}$  ions ( $3d^{10}$ ,  $S=0$ ) induce the strongest  $T_c$  reduction ( $\sim -12$  K/% Zn) [33,34]. Furthermore, low Zn substitution preserves the doping level and introduces only minimal structural disorder. We compare the spin excitation spectra reported from inelastic neutron scattering (INS) measurements performed in  $\text{YBa}_2(\text{Cu}_{1-y}\text{Zn}_y)_3\text{O}_7$  for various Zn/Cu substitution rates [6,11,20–22] (Characteristics of single crystals used for INS measurements are listed in Table I). Through Zn substitution, the magnetic resonance peak magnitude strongly decreases and its energy position slightly shifts to lower energy, so that the ratio  $E_r/T_c$  increases. In contrast to the Zn free system, where the normal state magnetic response is not experimentally discernible, nonmagnetic impurities restore or enhance AF spin fluctuations above  $T_c$  and up to  $\sim 250$  K.

## II. INS MEASUREMENTS

Throughout this review, the wave vector  $\mathbf{Q}$  is indexed in units of the reciprocal tetragonal lattice vectors  $2\pi/a = 2\pi/b = 1.63 \text{ \AA}^{-1}$  and  $2\pi/c = 0.53 \text{ \AA}^{-1}$ . In this notation the  $(\pi/a, \pi/a)$  wave vector parallel to the  $\text{CuO}_2$  planes corresponds to points of the form  $(h/2, k/2)$  with  $h$  and  $k$  odd integers. Because of the well known intensity modulation of the low energy spin excitations due to interlayer interactions [1–6], data were taken close to  $L=1.7 l$  where  $l$  is an odd integer.

In pure  $\text{YBa}_2\text{Cu}_3\text{O}_7$ , the magnetic resonance peak appears at  $E_r \sim 40$  meV [4]. Figure 1.a shows the difference between two energy scans, performed with a momentum transfer fixed at  $\mathbf{Q}_{\text{AF}}=(1.5, 0.5, 1.7)$ . The former is measured

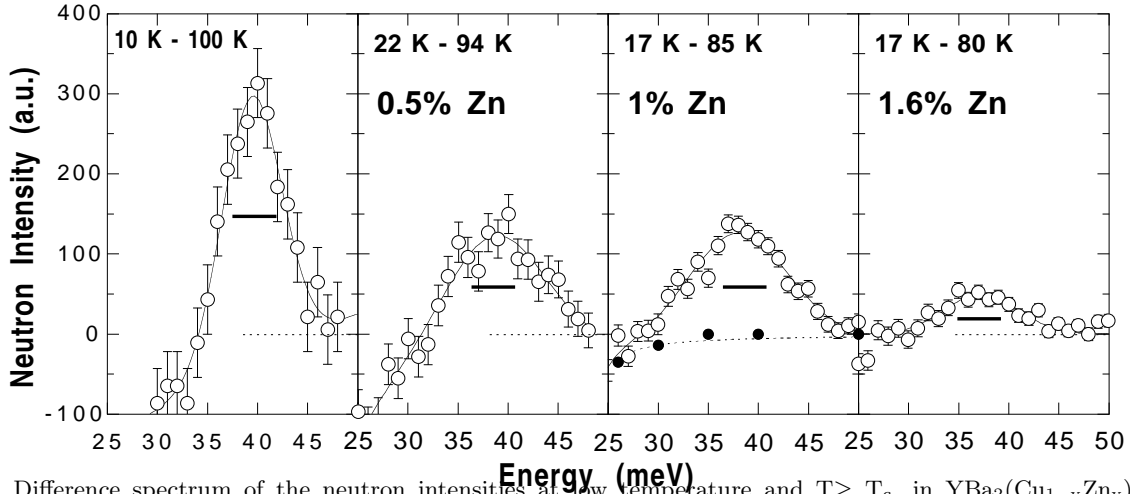


FIG. 1. Difference spectrum of the neutron intensities at low temperature and  $T \geq T_c$ , in  $\text{YBa}_2(\text{Cu}_{1-y}\text{Zn}_y)_3\text{O}_7$  (open symbols): a)  $y=0$  [4], b)  $y=0.005$  [20], c)  $y=0.01$  [11], d)  $y=0.016$ . Measurements have been normalized against phonons. Full symbols correspond to the reference level of magnetic scattering and is determined from the difference of constant-energy scans at both temperatures. This level becomes slightly negative with decreasing energy owing to the thermal enhancement of the nuclear background. Dotted lines are guides to the eye.

deep in the superconducting state and the latter, in the normal state, close to  $T_c$ . The magnetic resonance peak gives rise to a positive contribution to the difference spectrum, with a maximum at  $E_r$  (Fig. 1.a). Besides, a negative difference at low energy stems from phonon scattering (determined independently through constant-energy scans). The magnetic intensity has been converted to the imaginary part of the dynamical magnetic susceptibility,  $\chi''$ , after correction by the detailed balance and magnetic form factors and calibrated against optical phonons according to a standard procedure [20]. The maximum at  $E_r$  in Fig. 1.a then corresponds to an enhancement of  $\chi''$  at the AF wave vector (hereafter  $\Delta\chi''(\mathbf{Q}_{\text{AF}}, E_r)$ ) of  $\sim 300 \mu_B^2 \cdot \text{eV}^{-1}$ . A fit to a Gaussian profile of the positive part of the difference spectrum (Fig 1) provides an estimate of the energy distribution of  $\Delta\chi''(\mathbf{Q}_{\text{AF}}, E)$  around  $E_r$ . The full width at half maximum of the difference spectrum is  $\Delta E \sim 6$  meV, of the same order of magnitude as the instrumental resolution ( $\sim 5$  meV), yielding an intrinsic energy width of at most  $\sim 3$  meV. In  $\text{YBa}_2\text{Cu}_3\text{O}_7$ , the magnetic resonance peak is thus almost resolution limited in energy [3,4,6]. The temperature dependence of  $\chi''(\mathbf{Q}_{\text{AF}}, 40 \text{ meV})$ , shown in Fig. 2.a [5], exhibits a marked change at  $T_c$ , and an order-parameter-like curve in the superconducting state: the telltale signature of the resonance peak. Above  $T_c$ , magnetic fluctuations are not sizeable anymore. According to Ref. [4,16], the magnitude of spin fluctuations left above  $T_c$  cannot exceed  $\sim 70 \mu_B^2 \cdot \text{eV}^{-1}$ . At 40 meV, the ratio,  $R$ , between the intensities of AF spin fluctuations above  $T_c$  and at low temperature ranges from 0 to  $\sim 20\%$  (see Table. I).

The same kind of INS measurements have been performed on Zn substituted  $\text{YBa}_2\text{Cu}_3\text{O}_7$  samples. The difference spectrum of neutron intensities for each Zn content is determined from energy scans performed at wave vector  $\mathbf{Q}_{\text{AF}}=(-1.5, -0.5, 1.7)$ , following the procedure described above for the Zn free sample. For each Zn content, the difference spectra still exhibit a positive maximum around  $\sim 40$  meV (Fig. 1), that accounts for an enhancement of the magnetic response at low temperature. The intensity at the maximum drops down with increasing Zn substitution (Table I). Nonmagnetic impurities, that strongly reduce  $T_c$ , therefore significantly weaken the enhancement of the magnetic response in the superconducting state, ascribed to the magnetic resonance peak. The energy position of the maximum slightly moves to lower energy, giving rise to a progressive increase of the ratio  $E_r/T_c$  from  $\sim 5$  to  $\sim 6$ . In addition, the energy distribution  $\Delta E$  ( $\sim 8$  meV) broadens with Zn substitution, as compared to the difference spectrum of the Zn free sample (Fig. 1.a). The magnetic resonance peak thus exhibits an intrinsic energy width that accounts for a disorder induced broadening [11,20].

In  $\text{YBa}_2(\text{Cu}_{0.99}\text{Zn}_{0.01})_3\text{O}_7$ , the temperature dependence of  $\chi''(\mathbf{Q}_{\text{AF}}, 40 \text{ meV})$  shows an upturn at  $T_c$  and displays remnants of an order parameter lineshape in the superconducting state, that characterize the magnetic resonance peak (Fig. 2.b). The change of slope at  $T_c$  is hardly visible in the 0.5% and 2% Zn substituted samples [6,20] (where data quality is not as high). Indeed, the hallmark of the magnetic resonance peak in the temperature dependence of  $\chi''$  is partially scrambled by AF spin fluctuations in the normal state which are enhanced or restored by Zn. These fluctuations persist up to  $\sim 250$  K (Fig. 2). Close to 40 meV, their relative weight with respect to the magnetic intensity at low temperature,  $R$ , increases with increasing Zn substitution (Table I). Notice that the slight anomaly at  $T_c$  in the 1% Zn substituted sample is visible only because of the high quality of the data and that the improvement

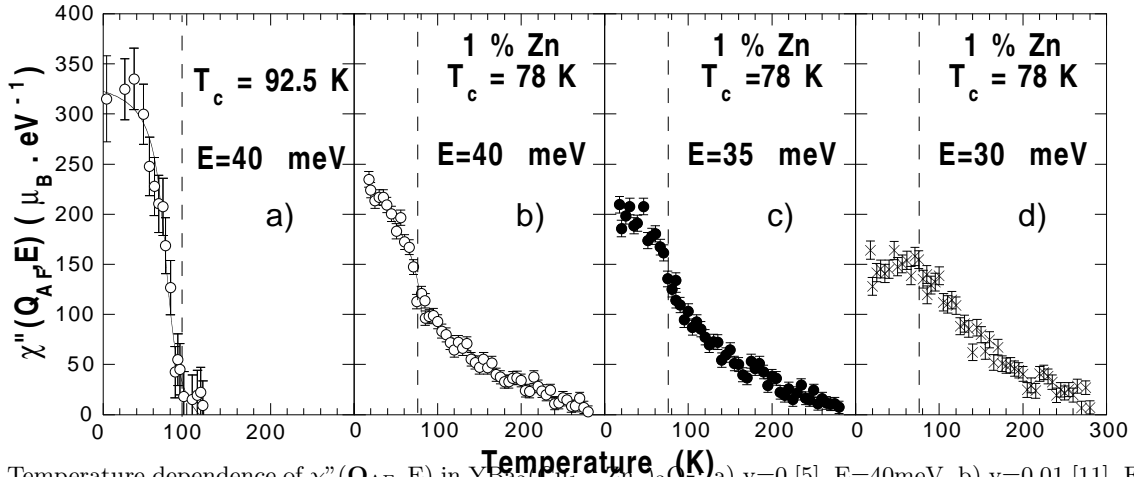


FIG. 2. Temperature dependence of  $\chi''(\mathbf{Q}_{AF}, E)$  in  $\text{YBa}_2(\text{Cu}_{1-y}\text{Zn}_y)_3\text{O}_7$ : a)  $y=0$  [5],  $E=40\text{meV}$ , b)  $y=0.01$  [11],  $E=40\text{ meV}$ , c)  $y=0.01$ ,  $E=35\text{ meV}$ , d)  $y=0.01$ ,  $E=30\text{ meV}$ . Data are given in absolute units. A  $\sim 30\%$  overall in absolute unit calibration is not included in the error bars. Solid lines are guides to the eye.

of data quality in other Zn substituted samples could reveal the same feature.

The temperature dependence of  $\chi''(\mathbf{Q}_{AF}, E)$  has been measured at 30 meV and 35 meV in  $\text{YBa}_2(\text{Cu}_{0.99}\text{Zn}_{0.01})_3\text{O}_7$  (Fig. 2.c-d). In this system, the magnetic resonance peak appears precisely at 38 meV ( $\Delta E \simeq 8\text{ meV}$ ) and the enhancement of the magnetic response around  $T_c$  can be observed in the temperature dependences of  $\chi''$  at 35 meV and 40 meV (Fig. 2.b-d). On the contrary,  $\chi''(\mathbf{Q}_{AF}, 30\text{meV})$  saturates or even slightly decreases below  $T_c$ . A detailed analysis of Fig. 2.b-d reveals that the intensity of the magnetic response left in the normal state is actually larger at 30 and 35 meV than at 40 meV. This implies a possible redistribution of the magnetic spectral weight in the normal state.

Fig. 3.a-b show constant-energy scans at 40 meV in the  $(H, H/3, 1.7)$  zone at 17 K and 275 K. At low temperature, the magnetic response displays a Gaussian momentum distribution centered at the AF wave vector, on top of a background that is slightly curved due to a contribution from phonons. At 275 K, the magnetic response is not sizeable anymore (Fig. 3.a) and an energy scan performed at  $\mathbf{Q}_{AF}=(-1.5, -0.5, 1.7)$  characterizes the energy dependence of the background at high temperature (Fig. 3.c). In the energy range  $E=30\text{-}50\text{ meV}$ , its lineshape is well approximated by a third order polynomial fit of data at  $\{30, 35, 40, 50\}\text{ meV}$ . At lower temperature, the same fit of background intensities determined from a set of constant-energy scans at  $\{30, 35, 40, 50\}\text{ meV}$  defines an effective background (Fig. 3.d). Its subtraction from the raw intensity leads to the magnetic excitation spectrum (open symbols in Fig. 3.e). Figure 3.e shows the magnetic excitation spectrum at  $\mathbf{Q}_{AF}$  from 30 to 50 meV in  $\text{YBa}_2(\text{Cu}_{0.99}\text{Zn}_{0.01})_3\text{O}_7$ : in the superconducting state (17 K), close to  $T_c$  (85 K) and well above  $T_c$  (200 K). In the normal state, the maximum of  $\chi''(\mathbf{Q}_{AF}, E)$  moves inside the energy range 30-35 meV, whereas the maximum intensity is still peaked around  $\sim 38\text{ meV}$  in the superconducting state.

We can summarize the experimental observations in  $\text{YBa}_2(\text{Cu}_{1-y}\text{Zn}_y)_3\text{O}_7$  as follows. In the superconducting state, the magnetic resonance peak broadens in energy and slightly moves to lower energy, but remains located close to  $\sim 40\text{ meV}$ , the energy position of the resonance peak in pure  $\text{YBa}_2\text{Cu}_3\text{O}_7$ . A broad peak with a characteristic energy

$y$ (%)	$V$ ( $\text{cm}^3$ )	$T_c$ (K)	$E_r$ (meV)	$\Delta\chi''$ ( $\mu_B^2 \cdot \text{eV}^{-1}$ )	R (%)	Ref.
0	10	93	40	$\sim 300$	$\leq 20$	[4]
0.5	1.7	87	39	$\sim 130$	$\sim 50$	[20]
1	$\sim 2$	78	38	$\sim 130$	$\sim 50$	[11]
1.6	$\sim 2$	73	37	$\sim 50$	-	-
2	0.2	69	-	-	$\geq 70$	[21,6]

TABLE I.  $\text{YBa}_2(\text{Cu}_{1-y}\text{Zn}_y)_3\text{O}_7$  single crystals used in INS measurements: (a) Zn content,  $y$ , (b) volume,  $V$ , (c) superconducting critical temperature,  $T_c$ . The samples were heat-treated to achieve full oxygenation and the Zn/Cu substitution rate was deduced from the reduction of  $T_c$  as compared to the pure system. In each sample, the magnetic resonance peak can be characterized by the following parameters: (d) the energy position,  $E_r$ , (e) the enhancement, between  $T \rightarrow 0$  and  $T_c$ , of dynamical spin susceptibility at  $E_r$  and  $\mathbf{Q}_{AF}$ ,  $\Delta\chi''(\mathbf{Q}_{AF}, E_r)$ . R corresponds to the ratio between AF intensities left just above  $T_c$  and at low temperature:  $R = \chi''(\mathbf{Q}_{AF}, E_r)_{T_c} / \chi''(\mathbf{Q}_{AF}, E_r)_{T \rightarrow 0}$ . R is given at 39 or 40 meV. (for further details, see text)

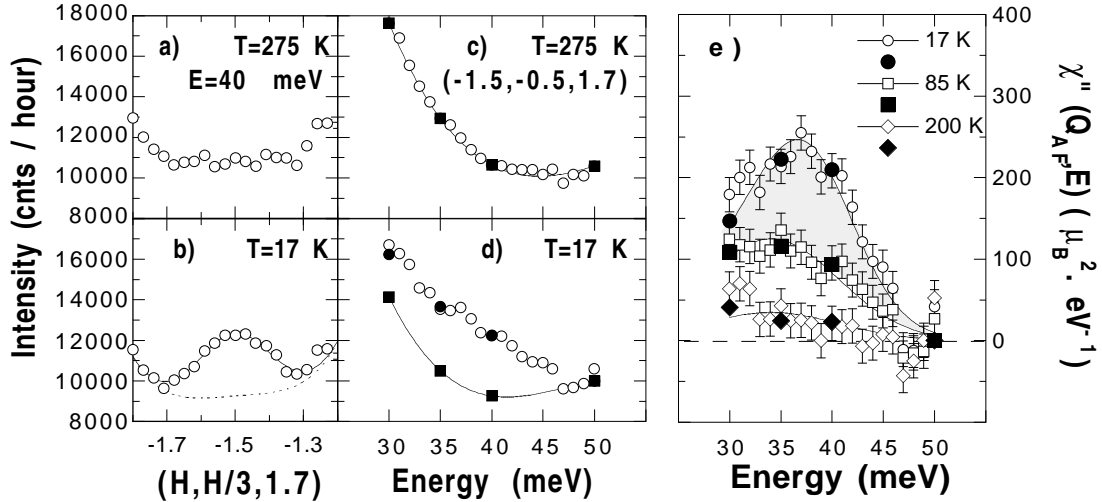


FIG. 3.  $\text{YBa}_2(\text{Cu}_{0.99}\text{Zn}_{0.01})_3\text{O}_{7-\delta}$ . Constant energy scans at 40 meV in the (H,H/3,1.7) zone: a) 275 K, b) 17 K). Energy scan at the wave vector (-1.5,-0.5,1.7): c) 275 K, d) 17 K). Full circles and squares account for the magnetic intensity and background intensities determined from constant energy scans at different energies. The lineshape of the background is fitted to a third order polynomial function. e)  $\chi''(\mathbf{Q}_{AF}, E)$  in the energy range 30-50 meV, at different temperatures. The shaded area corresponds to  $\Delta\chi''(\mathbf{Q}_{AF}, E)$  reported in Fig.1.c. Solid lines are guides to the eye.

comparable to (but somewhat lower than) the energy of the resonance peak appears in the normal-state response of Zn-substituted systems. While the normal state AF spin fluctuations develop with increasing Zn substitution, the enhancement of the magnetic response, associated with magnetic resonance peak in the superconducting state, fades away.

### III. DISCUSSION AND CONCLUSION

A comparison of our measurements in the pure YBCO system with current models of the spin dynamics in cuprates is given in [10]. However, most of these models do not incorporate disorder. Here we restrict the discussion to theoretical works where the interplay between (collective) spin excitations and quantum impurities in high temperature superconductors is expressly considered.

In BCS d-wave superconductors, nonmagnetic impurities cause the decay of the quasi-particle states due to a strong scattering rate (close to the unitary limit), and then, give rise to a pair breaking that reduces strongly the superconducting order parameter [23–32]. The resonant scattering by non magnetic impurities qualitatively account for most of the Zn substitutions effects in High- $T_c$  superconductors: i) the strong alteration the bulk superconducting properties, such as the critical temperature [33,34] and the superfluid density [35,36], ii) the increase of the in-plane residual resistivity, iii) the reduction of the microwave surface resistance [37] and iv) the appearance of a finite density of state at the Fermi level below  $T_c$  [38]. Therefore, as a consequence of the reduction of the superconducting order parameter, the threshold of the electron hole spin flip continuum at the AF wave vector moves in principle to low energy as, in the superconducting state, that threshold energy is basically proportional to twice the maximum of the d-wave gap. Thus, in any models where the resonance appears at or below the continuum threshold, nonmagnetic impurities should lead to a shift of the resonance to lower energy and the occurrence of damping (so that no clear resonance is observed at large impurity concentrations) [39,40]. These results provide an explanation for the broadening of the magnetic resonance peak. Similar broadening can also occur due to disorder in the paramagnetic state of quantum antiferromagnet [41]. However, the magnitude of the  $E_r$ -renormalization strongly depends on the model used to account for the magnetic resonance peak in the Zn-free system, and then, would be important to discriminate between the different models for the magnetic resonance peak. Furthermore, the strong scattering by non magnetic impurities, so crucial in the superconducting state, also modifies the normal state properties. In the normal state, the effect of nonmagnetic impurities on the the spin fluctuation spectral weight at the AF wave vector has been studied in the framework of the the 2D Hubbard model using the random phase approximation [42]. The main effect of dilute impurities on the noninteracting dynamical spin susceptibility is a weak smearing. On the contrary, for an interacting system, the scattering of spin fluctuations by the (static and extended [43]) impurity potential with a finite momentum

transfer ("umklapp" processes) becomes essential. Indeed, the  $(\pi/a, \pi/a)$  spin fluctuations become mixed with other wave vector components, and a new peak in  $\chi''(\mathbf{Q}_{AF}, \omega)$  can appear.

Scanning tunneling microscopy (STM) in Zn substituted  $\text{Bi}_2\text{Sr}_2\text{CaCu}_2\text{O}_{8+\delta}$  [44] confirms the existence of a strong quasi-particle scattering rate by impurities. Indeed, STM shows intense quasi-particle scattering resonances at Zn sites, coincident with strong suppression of the superconducting coherence peaks at the Zn site. Furthermore, the superconducting peaks then are progressively restored over a distance,  $\xi$ , of about 15 Å. STM supports the proposal that the superfluid density reduction can be explained by non-superconducting regions of area  $\sim \pi\xi^2$  around each impurity atoms, the so-called "Swiss cheese" model, introduced to account for the decrease of the superconducting condensate density from  $\mu\text{SR}$  measurements [35]. On a phenomenological level, our data are actually consistent with this scenario in which Zn impurities are surrounded by extended regions in which superconductivity never develops [35,44]. Within this picture, superconductivity is then confined to (perhaps only rather narrow) regions far from the Zn impurities. This would explain why Zn impurities all but eradicate the effect of superconductivity on the spin excitations which is so readily apparent in the pure system. Since INS is a bulk measurement and the magnetic resonance peak is an intrinsic feature of the superconducting state, one may speculate that its intensity may be suppressed as the fraction of the system that becomes superconducting and, thus, may scale with the superfluid condensate density. In addition, in non-superconducting regions around Zn impurities, magnetic properties are strongly modified already far above  $T_c$ . According to nuclear magnetic resonance measurements, local magnetic moments develop on Cu sites surrounding a Zn impurity (up to the third nearest neighbors) [45].

The modification of the local magnetic properties and the resonant scattering from Zn impurities arise in a natural way from the strong correlation of the host as shown in exact diagonalizations of small clusters performed on the framework of the t-J model [46,47,43,48,49]. According to these calculations, electrons form a bound state around the impurity site and the magnitude of the local moment is enhanced, as observed experimentally [45,34]. When  $J/t$  becomes larger than  $\sim 0.3$ , a mobile hole is trapped by the impurity potential induced by the local distortion of the AF background. Below  $T_c$ , a pair breaking effect occurs due to the binding of holes to the impurity. Likewise, a new magnetic excitation corresponding to the singlet-triplet excitation of the singlet impurity-hole bound state is predicted [49]. The nucleation of staggered magnetic moment where superconductivity is suppressed and/or the singlet-triplet excitation of the singlet impurity-hole bound state [49] may contribute to the a broad peak observed in the normal state up to  $\sim 250$  K, with a characteristic energy smaller than  $E_r$  (but of the same order of magnitude). In this picture, the magnetic resonance peak and spin fluctuations intrinsic to Cu spins surrounding Zn impurities coexist in the superconducting state.

In conclusion, our INS data show that the interplay between non magnetic quantum impurities and spin dynamics in the cuprates is a surprisingly rich field of investigation, that emphasized the importance of strong correlation and the competition between the superconducting ground state and antiferromagnetism. We hope that this review will stimulate further theoretical and experimental work.

## ACKNOWLEDGMENTS

The authors wish to acknowledge P. Hirschfeld, J. Bobroff, P. Pfeuty and F. Onufrieva for helpful discussions.

- 
- [1] J. Rossat-Mignod *et al.*, Physica C **185-189**, 86 (1991).
  - [2] H.A. Mook *et al.*, Phys. Rev. Lett. **70**, 3490 (1993).
  - [3] L. P. Regnault *et al.*, Physica C **235-240**, 59 (1994); Physica B **213-214**, 48 (1994).
  - [4] H.F. Fong *et al.*, Phys. Rev. Lett. **75**, 316 (1995); Phys. Rev. B **54**, 6708 (1996).
  - [5] P. Bourges *et al.*, Phys. Rev. B **53**, 876 (1996).
  - [6] L. P. Regnault *et al.*, in *Neutron Scattering in Layered Coper-Oxide Superconductors*, A. Furrer (Kluwer, Amsterdam, 1998), p 85.
  - [7] P. Dai *et al.*, Phys. Rev. Lett. **77**, 5425 (1996).
  - [8] H.F. Fong *et al.*, Phys. Rev. Lett. **78**, 713 (1997).
  - [9] P. Bourges *et al.*, Europhys. Lett. **38**, 313 (1997).
  - [10] H.F. Fong *et al.*, Phys. Rev. B **61**, 14774 (2000).
  - [11] Y. Sidis *et al.*, Phys. Rev. Lett. **84**, 5900 (2000) (cond-mat/9912214).

- [12] H.F. Fong *et al.*, Nature **398**, 588 (1999).
- [13] H. He *et al.*, cond-mat/0002013.
- [14] P. Dai *et al.*, Phys. Rev. Lett. **80**, 1738 (1998).
- [15] H.A. Mook *et al.*, Nature **395**, 580 (1998).
- [16] P. Bourges *et al.*, in *High Temperature Superconductivity* S.E. Barnes *et al* Eds. (CP483 AIP, Amsterdam, 1999) pp 207-212 (cond-mat/9902067).
- [17] M. Arai *et al.*, Phys. Rev. Lett. **83**, 608 (1999).
- [18] P. Bourges *et al.*, Science **288**, 1234 (2000); cond-mat/0006085.
- [19] F. Onufrieva and P. Pfeuty, cond-mat/9903097.
- [20] H.F. Fong *et al.*, Phys. Rev. Lett. **82**, 1939 (1999).
- [21] Y. Sidis *et al.*, Phys. Rev. B **53**, 6811 (1996).
- [22] Y. Sidis *et al.*, Int. J. Mod. Phys. B **12**, 3330 (1998).
- [23] D. Poilblanc *et al.*, Solid. St. Com **59**, 111 (1986).
- [24] L.S. Borkowski *et al.*, Phys. Rev. B **49**, 15404 (1994).
- [25] T. Hotta *et al.*, Phys. Rev. B **62**, 274 (1993).
- [26] Y. Sun *et al.*, Phys. Rev. B **51**, 6059 (1994).
- [27] A.V. Balatsky *et al.*, Phys. Rev. B **51**, 15547 (1995).
- [28] H. Kim *et al.*, Phys. Rev. B **52**, 13576 (1995).
- [29] R. Fehrenbacher, Phys. Rev. Lett. **77**, 1849 (1996).
- [30] A.V. Balatsky and M.I. Salkola, Phys. Rev. Lett. **76**, 2386 (1996).
- [31] M. Franz *et al.*, Phys. Rev. B **54**, R6887 (1996).
- [32] G. Harañ *et al.*, condmat/9904263.
- [33] M. Tarascon *et al.*, Phys. Rev. B **37**, 7458 (1988).
- [34] P. Mendels *et al.*, Europhysics Lett. **46**, 678 (1999).
- [35] B. Nachumi *et al.*, Phys. Rev. Lett. **77**, 5421 (1996).
- [36] C. Bernhard *et al.*, Phys. Rev. Lett. **77**, 2303 (1996).
- [37] D.A. Bernhard *et al.*, Phys. Rev. B **50**, 4051 (1994).
- [38] K. Ishida *et al.*, Physica C **179**, 29 (1991); J. Phys. Soc. Jpn **62**, 2803 (1993).
- [39] J.X. Li *et al.*, Phys. Rev. B **58**, 2895 (1998).
- [40] D. Morr and D. Pines, Phys. Rev. Lett. **81**, 1086 (1998).
- [41] M. Vojta *et al.*, Phys. Rev. B **61**, 15152 (2000) (cond-mat/9912020).
- [42] N. Bulut, cond-mat/9909437, cond-mat/9908266.
- [43] W. Ziegler *et al.*, Phys. Rev. B **53**, 8704 (1996).
- [44] S.H. Pan *et al.*, Nature **403**, 748 (2000).
- [45] V. A. Mahajan *et al.*, Phys. Rev. Lett. **72**, 3100 (1994).
- [46] D. Poilblanc *et al.*, Phys. Rev. Lett **72**, 884 (1994); Phys. Rev. B **50**, 13020 (1994).
- [47] Y. Ohta *et al.*, Physica C **263**, 94 (1996).
- [48] S. Odashima *et al.*, Phys. Rev. B **56**, 126 (1997).
- [49] J. Riera *et al.*, Phys. Rev. B **54**, 7441 (1996).